Journal of
Ceramic Science
and Technology

J. Ceram. Sci. Technol., **08** [4] 455-462 (2017)
DOI: 10.4416/JCST2016-00079
available online at: http://www.ceramic-science.com
© 2017 Göller Verlag

Effect of Alumina-Coated Graphite (ACG) on the Microstructure and Mechanical Properties of Al_2O_3-C Refractories

X. Xu, Y. Li*, Q. Wang, S. Sang, L. Pan

The State Key Laboratory of Refractories and Metallurgy, Wuhan University of Science & Technology, Wuhan 430081, PR China

received October 7, 2016; received in revised form June 17, 2017; accepted June 26, 2017

Abstract

Alumina-coated graphite (ACG) was prepared by soaking expanded graphite (EG) in an $AlCl_3$ solution with vacuum impregnation. The graphite was then filtered, dried and treated in a coke bed at 400 – 1000 °C. The ACG was incorporated into Al_2O_3-C refractories, partly or completely replacing EG. The results showed that the alumina coating on the graphite was effective and delayed the oxidation behavior of the expanded graphite. It also allowed the structure of the graphite to survive largely intact at high temperatures as it had been incorporated into the Al_2O_3-C refractories while there were fewer *in situ*-formed ceramic phases in the matrix, e.g. SiC whiskers. As a result, ACG-containing Al_2O_3-C refractories exhibited better thermal shock resistance than that of common Al_2O_3-C refractories.

Keywords: Alumina-coated graphite, expanded graphite, microstructure, mechanical properties

I. Introduction

Low-carbon-containing refractories were developed to meet the requirements for clean steel-making in the metallurgical industry. Several nanocarbon sources, e.g. carbon black [1], carbon nanotubes [2,3], graphene oxide nanosheets [4] were characterized with unique morphologies and specific properties to be used as raw materials for carbon-containing refractories. Relative to the carbon sources mentioned above, expanded graphite was regarded as a parallel assembly of countless graphene or graphene oxide nanosheets (GON_S), so it could wrap up aggregates to enhance their mechanical properties. Moreover, its vermicular porous structure and high compressibility and resilience contributed to the thermal shock resistance of refractories in service because it could absorb and release thermal stress [5,6,7]. However, the expanded graphite suffered serious structural alteration at high temperatures owing to its high reactivity [6,8]. So, it was necessary to inhibit the structural evolution of expanded graphite at high temperatures as much as possible in order to maintain good thermal shock resistance of low-carbon-containing refractories in service.

Recently, researchers have focused on repairing defects and coating carbon sources, e.g. methane plasma restoration [9], boron and nitrogen-doping [10,11] for repairing the defects as well as silica or alumina coating on graphene oxide [12,13]. For example, a new combination mode like B-C and B-O-C bonds formed in the structure of expanded graphite after boric acid was used to soak expanded graphite and the reaction between the product of boric acid decomposition and the carbon atoms in the defects in following treatment [14]. In addition, the hydrolysis of tetraethoxysilane in solution was employed to form a coating on graphene oxide. And SiO_2-graphene oxide (SiO_2-GO) was added to composite materials to improve the interfacial bonding strength between the graphene oxide (GO) and the matrix as well as the oxidation resistance of inorganic polymer materials [12].

In the present work, expanded graphite was first soaked in $AlCl_3$ solution with vacuum impregnation. It was then filtered, dried, and treated in a coke bed at 400 – 1000 °C to produce an alumina oxide coating on the graphite layer. In fact, numerous negative-charged oxygenic functional groups like hydroxyl and carboxyl existed on hexagonal grid defects of expanded graphite [15], so metal cations in the solution were enriched on the layer of graphene oxide under the attraction of opposite charges and adsorption of graphite layer with large specific surface area [16]. As a result, nano-alumina particles coated the surface of graphene oxide nanosheets to improve the oxidation resistance of expanded graphite. At the same time, the coating allowed the structure of expanded graphite to survive largely intact at high temperatures for thermal shock resistance as it was incorporated into Al_2O_3-C refractories.

II. Experimental Procedure

(1) Preparation of ACG

Expanded graphite (EG) was first prepared by rapid heating of expandable graphite oxide (50 mesh, > 98 wt% fixed carbon, Shandong) placed in an iron saggar at 900 °C for 60 s in a muffle and then it was soaked in 1 mol/L $AlCl_3$ solution ($AlCl_6{\cdot}6H_2O$ > 97 wt%, Sinopharm chemical reagent Co., Ltd) with vacuum impregnation for 30 min. After filtering and drying at 110 °C for 24 h, the

* Corresponding author: liyawei@wust.edu.cn

precursor of alumina-coated graphite (ACG) was obtained. Subsequently, this was treated in a coke bed at 400 °C, 600 °C and 1000 °C with a holding time of 3 h, respectively to prepare the alumina coating on the expanded graphite.

(2) Preparation of Al_2O_3-C refractory specimens

In this experiment, tabular alumina (3 – 1 mm, 1 – 0.5 mm, 0.5 – 0 mm, 45 μm and 20 μm, 99.5 wt% Al_2O_3, Qingdao Almatis Premium Alumina Co., Ltd., China), α-Al_2O_3 (2 μm, 99 % Al_2O_3, Kaifeng Special Refractories Co., Ltd., China), aluminum powder (< 74 μm, 99 % Al, Xinxiang, China), silicon powder (< 45 μm, 98.47 wt% Si, Anyang, China), microsilica powder (0.5 μm, 97 wt% SiO_2, Elkem, Norway) were used as raw materials to prepare Al_2O_3-C refractories. In addition, thermosetting phenolic resin (liquid, > 40 % fixed carbon, Wuhan Lifa Chemistry & Industry CO., Ltd., China) was added as a binder. The reference batch composition (named E1) consisted of 83 wt% tabular alumina, 10 wt% α-Al_2O_3, 2 wt% Al powder, 3 wt% Si powder, 1 wt% microsilica powder and 1 wt% EG. 0.5 wt% and 1 wt% ACG coked at 1000 °C were used to partly or totally replace the EG as the carbon source in batch compositions (named EA0.5 and EA1, respectively) in a total addition amount of 1 wt% graphite. The refractory specimens were prepared as follows: All the batches were mixed for 30 min in the mixer After kneading, bar-shaped specimens were compacted into 25 mm in width, 25 mm in height and 140 mm in length at a pressure of 150 MPa and cured at 140 °C for 24 h. Finally, all specimens were coked at 1000 °C, 1200 °C, 1400 °C with a holding time of 3 h, respectively, and then cooled to room temperature.

(3) Testing and characterization

The phase compositions of original expanded graphite, the precursor of ACG, ACG coked at 400 °C, 600 °C, 1000 °C and Al_2O_3-C specimens were analyzed by means of X-ray diffraction (XRD, x'Pert Pro, Philips, Netherlands) and their microstructures were observed with transmission electron microscopy (TEM-2100 UHR STEM/EDS JEOL). The functional groups of the original expanded graphite and the precursor of ACG were investigated with a FT-IR spectrometer (IS50 FT-IR, Thermo Scientific, USA). The oxidation resistance of the ACG was examined by means of thermogravimetric analysis (TG-DSC, STA499, NETZSCH, Germany) in air atmosphere.

The cold modulus of rupture (CMOR) of the Al_2O_3-C specimens was measured in the three-point bending test at ambient temperature with a span of 100 mm and a loading rate of 0.5 mm/min using an electronic digital control system (EDC 120, DOLI Company, Germany) while the force-displacement curves were recorded simultaneously. The elasticity modulus (E) of all bar-shaped specimens was determined with a resonance frequency and damping analyzer (RFDA, IMCE in Belgium) at room temperature. Besides, the ruptured specimens were observed with a field emission scanning electron microscope (FESEM, Nova 400 NanoSEM, FEI Company, USA).

Moreover, the thermal shock resistance of specimens coked at 1200 °C was tested with the oil quenching method. After five thermal shock cycles, the mechanical properties of the specimens were measured in the three-point bending test. The residual strength ratio of CMOR was calculated based on the change of CMOR before and after the thermal shocks, i.e. the residual strength ratio of CMOR = 100 × $CMOR_{TS}$/CMOR, where CMOR and $CMOR_{TS}$ were the CMOR before and after five thermal shock cycles, respectively.

III. Results and Discussion

(1) Alumina-coated graphite (ACG)

(a) *FT-IR*

With regard to the original expanded graphite, several types of oxygen functionalities were present in the FT-IR spectrum (Fig. 1). The peak at 3473 cm^{-1} was attributed to the O-H stretching vibrations of the C-OH groups and water. The peak at 1714 cm^{-1} was assigned to C=O groups located at the edges of the graphite layer [15]. The peak at 1622 cm^{-1} was related to aromatic C=C bonds [17,18]. Compared with original expanded graphite, a broader peak between 3000 cm^{-1} and 3700 cm^{-1} appeared in the precursor of ACG, which might be influenced by the O-H stretching vibrations of water and Al-OH generated by the partial hydrolysis of aluminum ions [19]. In addition, the stretching vibrations peak of Al-Cl appeared at 602 cm^{-1} [20]. With the increase in temperature, the stretching vibration peak of Al-Cl disappeared and the peak intensity of O-H stretching vibrations decreased. In addition, the characteristic absorption band of alumina appeared in the range of 400 – 1000 cm^{-1} and became obvious for ACG treated at 1000 °C [21,22].

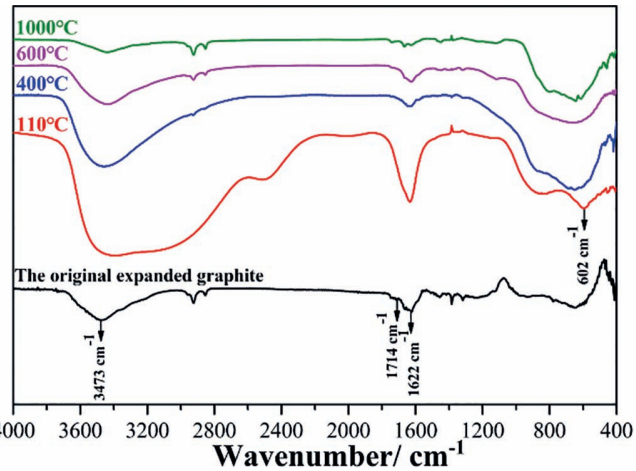

Fig. 1: FTIR spectra of the precursor of ACG coked at 400 – 1000 °C.

(b) *XRD*

X-ray diffraction patterns of the precursor of ACG coked at 400 °C, 600 °C and 1000 °C were shown in Fig. 2. $AlCl_3 \cdot 6H_2O$ and graphite phases as main phase compositions appeared in the precursor of ACG. However, $AlCl_3 \cdot 6H_2O$ disappeared leaving the graphite after treatment at 400 °C and 600 °C in a coke bed. With the increase in temperature to 1000 °C, α-Al_2O_3 phase appeared in the

product. It was supposed that amorphous Al_2O_3 in the product transformed into α-Al_2O_3 at 600 – 1000 °C [23].

(c) ***TEM***

TEM was applied to observe the microstructure of the original EG and precursor of ACG coked at 400 °C, 600 °C and 1000 °C, respectively (Fig. 3). As for the original EG, it exhibited a smooth, transparent surface and its lattice fringes were clearly seen on the edge of graphite layers (Fig. 3(a)). After the dipping and drying process, amorphous substance was uniformly distributed on the surface of graphite nanosheets of EG except that a small amount of it collected on the fold and edges of graphite layer (Fig. 3(b)). Energy dispersive spectrum (EDS) showed that this amorphous substance contained Al, O, C, Cl elements. After treatment at 400 °C, amorphous substance containing Al, O, C elements uniformly coated the surface of graphite nanosheets of EG (Fig. 3(c)), which was inferred to be amorphous Al_2O_3. With the temperature rising up to 600 °C, Al_2O_3 particles with poor crystallinity and unobvious lattice fringe formed on the surface of graphite layer (Fig. 3(d)). Up to 1000 °C, Al_2O_3 formed in columnar and granular shapes and their lattice fringe was clearly observed (Fig. 3(e)).

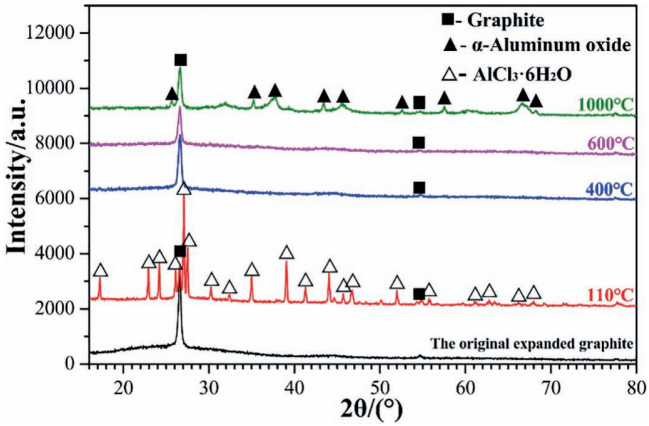

Fig. 2: XRD patterns of precursor of ACG coked at 400 – 1000 °C.

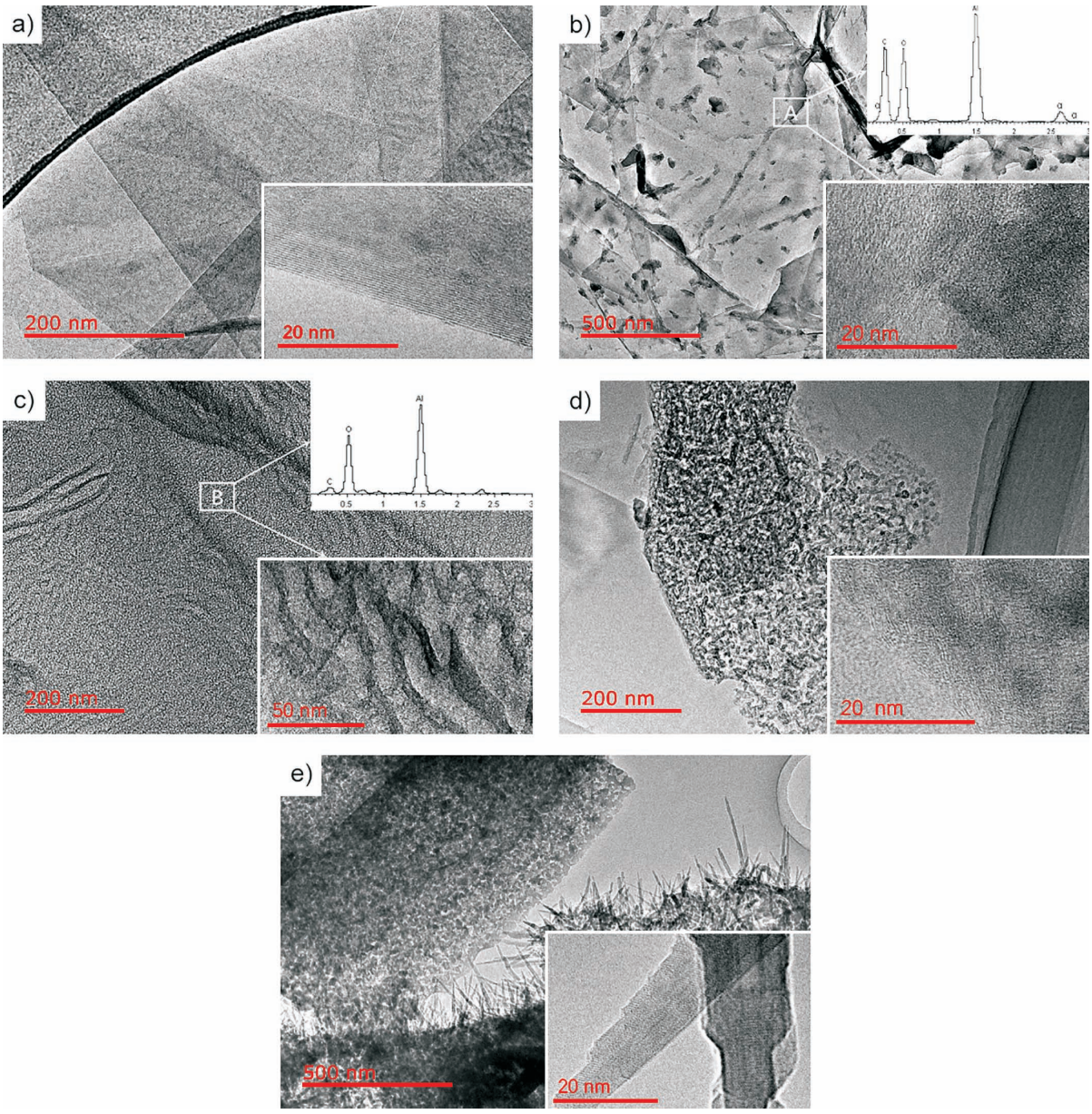

Fig. 3: TEM micrographs of original EG(a), precursor of ACG (b), ACG coked at 400 °C (c), 600 °C (d), 1000 °C (e).

(d) ***Thermal analysis***

TG and DSC curves of the original EG, the precursor of ACG and ACG coked at 400 °C, 600 °C and 1000 °C were shown in Fig. 4. For the precursor of ACG, weight loss occurred before 110 °C owing to the evaporation of free water. With the increase in temperature, the weight loss continued and an obvious endothermic peak appeared near 160 °C resulting from the decomposition of $AlCl_3 \cdot 6H_2O$. The weight loss in the range of 200 °C – 400 °C might be related to the decomposition of oxygen-containing functional groups on the expanded graphite and removal of structural water from the hydration products of aluminum. As the temperature rose, the precursor of ACG gradually oxidized with the oxidation exothermic peak at 839 °C.

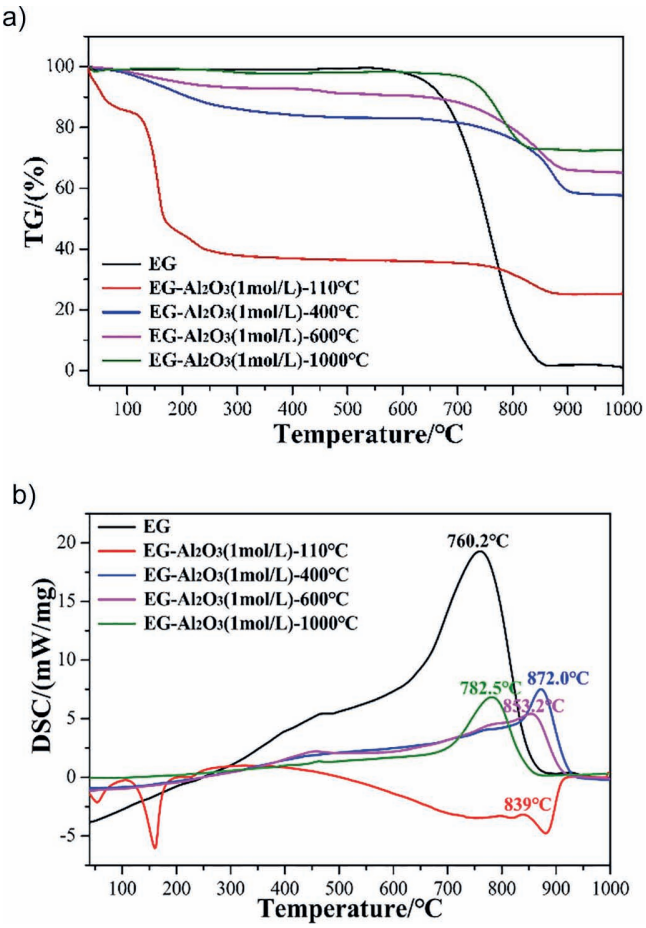

Fig. 4: TG (a) and DSC (b) curves of original EG, the precursor of ACG and ACG coked at 400 °C, 600 °C, and 1000 °C respectively.

For ACG treated at 400 °C – 1000 °C, the temperature corresponding to oxidation exothermic peak decreased from 872 °C to 782.5 °C with the increase of the heat treatment temperature, but it was still higher than that of the original expanded graphite (760.2 °C). Namely, the coating of aluminum oxide on the surface of graphite layers was helpful in delaying the oxidation behavior of the expanded graphite. In addition, the TG curves showed that the amount of alumina on the surface of the expanded graphite was close to 70 wt%, assuming complete oxidation of the expanded graphite in ACG.

(2) Al_2O_3-C refractories

(a) ***XRD***

Specimen E1 and EA1 coked at 1000 °C, 1200 °C and 1400 °C were examined with XRD in order to investigate the effect of ACG on phase evolution in the matrix of the Al_2O_3-C refractories at high temperatures (Fig. 5). Similar to specimen E1, corundum, graphite, Si, AlN and Al_4C3 phases were detected in the specimen EA1 coked at 1000 °C. With increase in temperature to 1200 °C, AlN, Al_4C3 phases disappeared and SiC phase appeared with the decrease of graphite and Si phase. Up to 1400 °C, the peak intensity of SiC phase increased slightly while the peak intensity of graphite phase decreased and Si phase disappeared completely. However, the peak intensity of ceramic phase such as AlN, Al_4C_3, SiC phase in specimen EA1 was lower than that of specimen E1 at the same coking temperature. In addition, it seemed that no significant decrease in amount was basically observed in the peak intensity of graphite phase in specimen EA1 after treatment at all high temperatures.

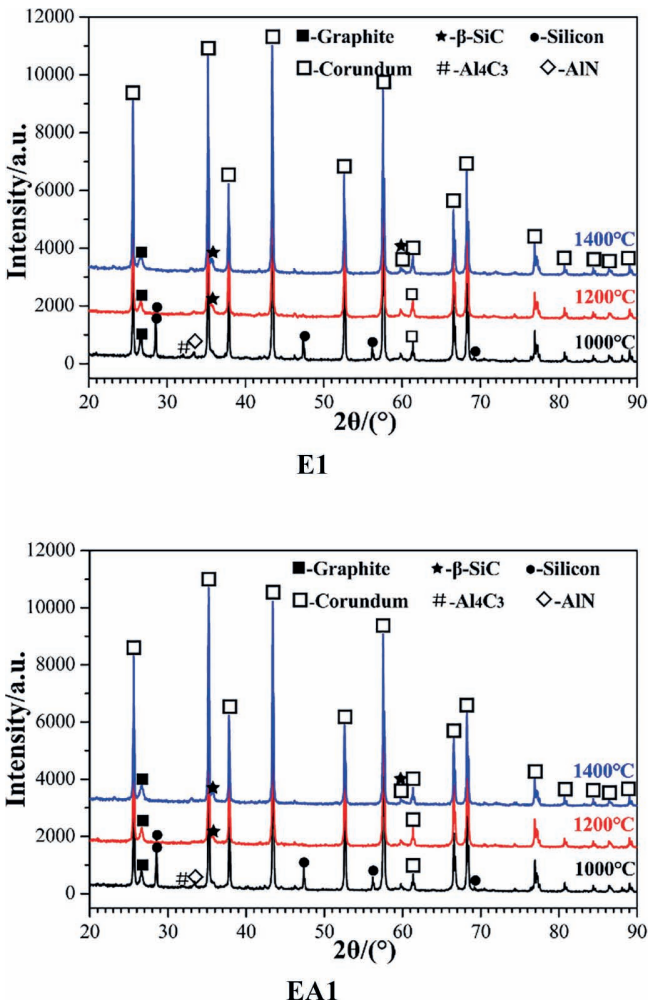

Fig. 5: XRD patterns of specimen E1 and EA1 coked at 1000 – 1400 °C.

(b) ***Microstructure***

The ruptured morphology of specimens E1 and EA1 coked at 1000 °C, 1200 °C and 1400 °C were also observed to investigate the effect of ACG on the microstructure

of Al_2O_3-C refractories (Fig. 6 and Fig. 7). With regard to specimen E1, an abundance of short column-shaped ceramic phases was located on the original area of metal aluminum additive in the specimen at 1000 °C and confirmed as AlN and Al_4C_3 respectively with the aid of EDS and XRD. In addition, some torn expanded graphite was still observed in the matrix of the specimen (Fig.6(a)). At 1200 °C, curly β-SiC whiskers appeared at the cost of expanded graphite (Fig. 6(b)). Meanwhile, a mass of β-SiC whiskers with large-diameter ratio formed in the matrix (Fig. 6(c)). As the temperature rose to 1400 °C, many more β-SiC whiskers formed in the matrix around the expanded graphite, but the length-diameter ratio decreased (Fig. 6(d)). Similar regular evolution of microstructure was found in specimen EA1 coked at corresponding temperatures. However, it is worth mentioning that fewer AlN and Al_4C_3 ceramic phases were observed in specimen EA1 coked at 1000 °C (Fig. 7(a)). Besides, the alteration degree of ACG in the specimen EA1 was significantly lower than expanded graphite in specimen E1 after treatment at 1200 °C and 1400 °C respectively, while fewer β-SiC whiskers appeared in the matrix (Fig. 7(b) to Fig. 7(d)).

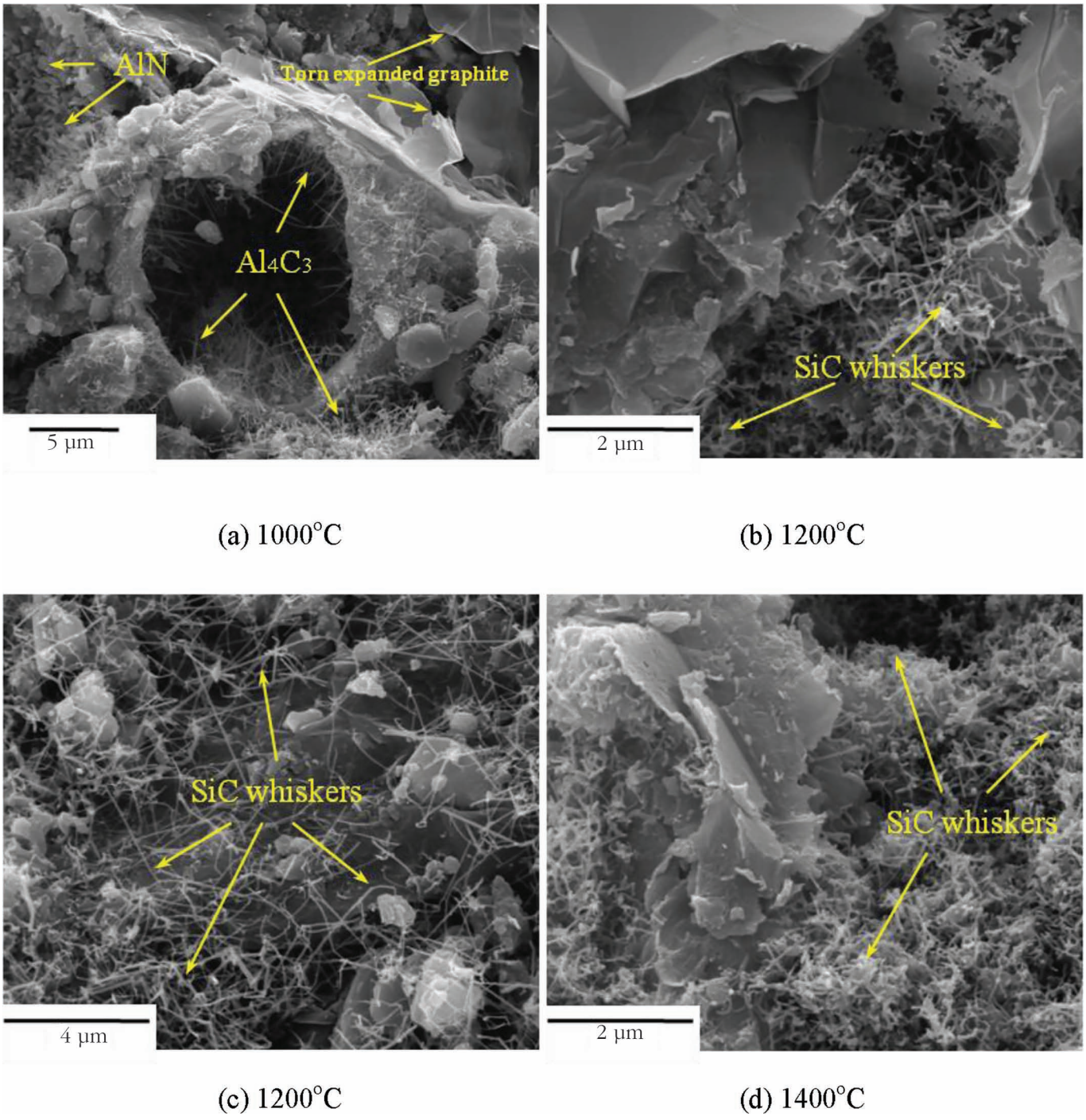

Fig. 6: SEM micrographs of E1 coked at (a) 1000 °C, (b) (c)1200 °C, (d) 1400 °C.

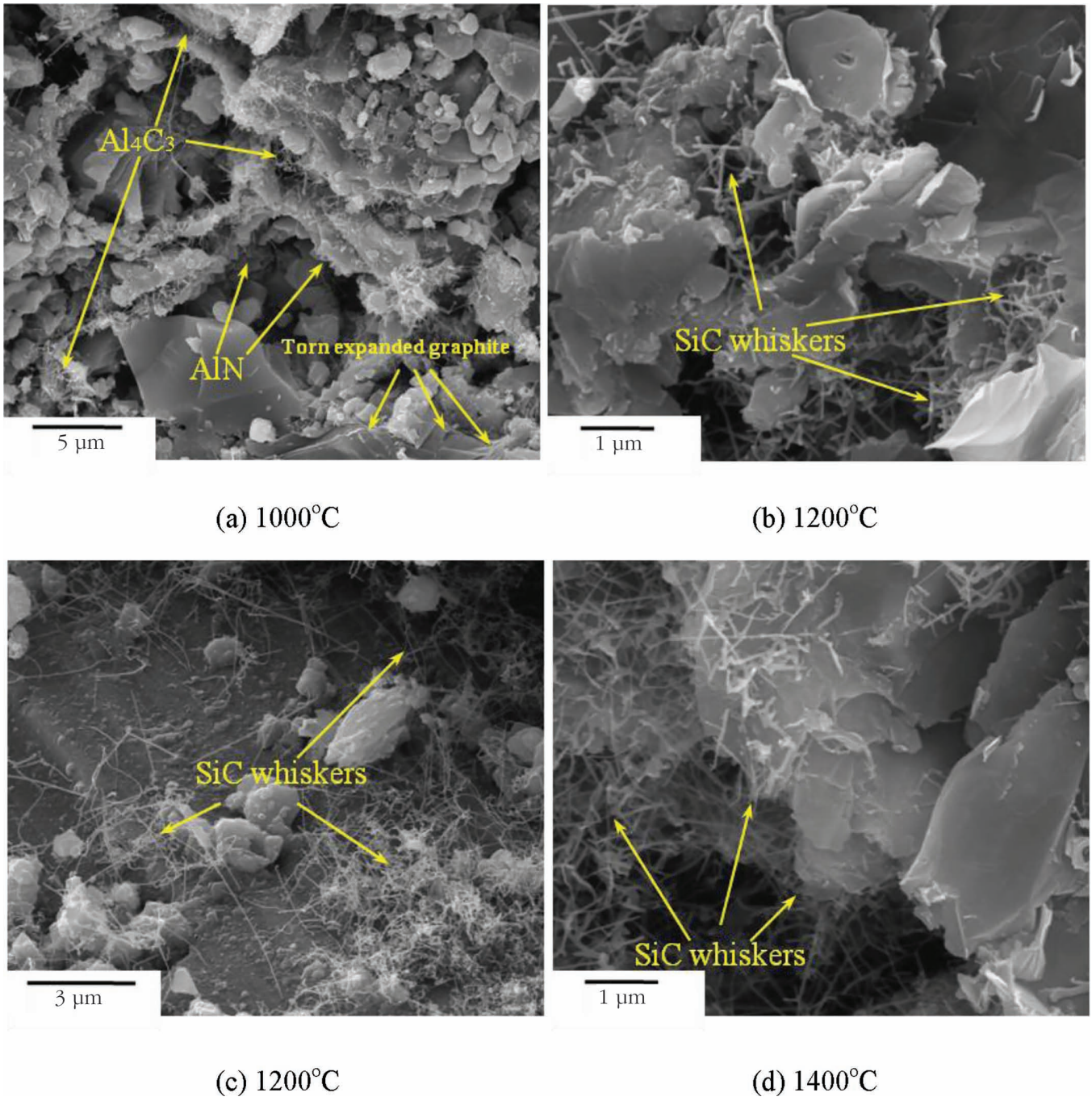

Fig. 7: SEM micrographs of EA1 coked at 1000 °C (a), 1200 °C (b, c) and 1400 °C(d).

(c) ***Mechanical properties***

The mechanical properties of specimens were closely related to the microstructure. Specimens E1, EA0.5 and EA1 coked at 1000 to 1400 °C were measured in a three-point bending test (Table 1). For all the specimens, the CMOR and E increased with the temperature from 1000 to 1200 °C, but decreased sharply at 1400 °C, which was in agreement with previous work [8, 24–26]. In specimen E1, EG with high reactivity promoted the formation of ceramic phases [6, 27–29], such as AlN, Al_4C_3 and SiC at 1000 to 1200 °C, which contributed to the improvement of the mechanical properties of the specimen. However, the expanded graphite underwent serious alteration at 1400 °C, which destroyed its integral structure although abundant β-SiC whiskers were produced at the template of the expanded graphite. Accordingly, the mechanical properties, e.g. CMOR of the specimen, dramatically reduced. In contrast to specimen E1, a lower CMOR was found in Al_2O_3-C refractories containing ACG coked at all the temperatures because the alumina coating on the graphite hindered the alteration of graphite, resulting in the integral structure of ACG in the matrix at high temperatures. The morphology of expanded graphite remained even at 1400 °C, but at the same time less ceramic phase formed in the matrix leading to the degradation of mechanical properties. In addition, the force-displacement curves of specimens in Fig. 8 show that the specimen coked at all the temperature possessed larger force-displacement and better fracture toughness as ACG was partly introduced into Al_2O_3 refractories.

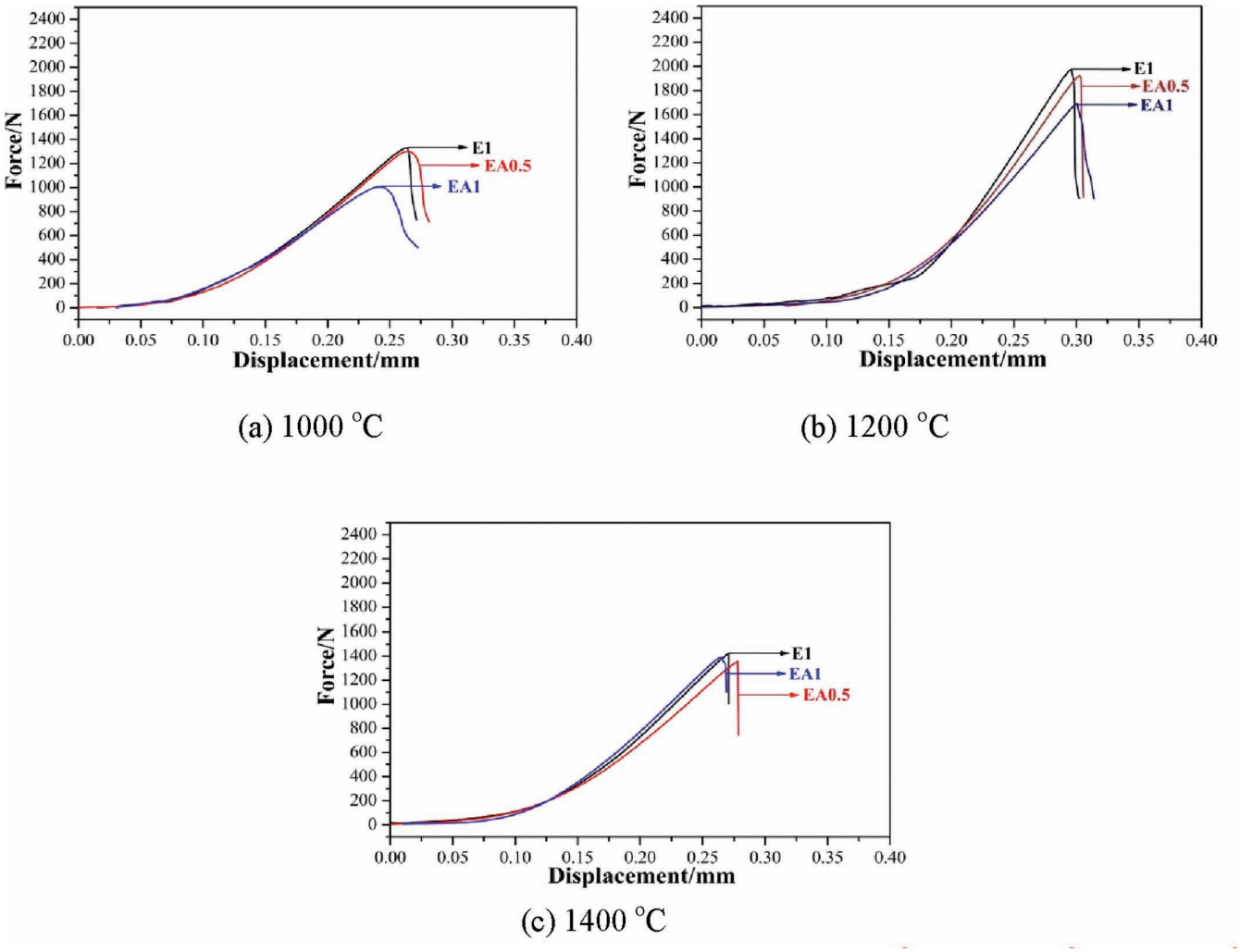

Fig. 8: Force-displacement curves of A_2O_3-C specimens coked at (a) 1000 °C, (b) 1200 °C, (c) 1400 °C.

Table 1: Cold modulus of rupture and elastic modulus of Al_2O_3-C specimens.

Temperature	Index	E1	EA0.5	EA1
1000 °C	CMOR (MPa)	12.95±0.28	11.80±0.12	9.94±0.33
	E (GPa)	38.95±0.62	33.22±1.10	23.72±1.82
1200 °C	CMOR (MPa)	19.73±0.21	19.43±0.18	16.89±0.34
	E (GPa)	64.59±1.82	60.65±1.13	46.81±1.87
1400 °C	CMOR (MPa)	13.45±0.13	13.14±0.15	13.33±0.13
	E(GPa)	43.89±1.08	42.02±1.26	40.13±1.14

(d) ***Thermal shock resistance***

The CMOR, $CMOR_{TS}$ and residual strength ratio of all the specimens were shown in Fig. 9. The CMOR of all the specimens decreased to a certain degree after the thermal shock test. However, it appeared that the incorporation of ACG into Al_2O_3-C refractories could improve the thermal shock resistance. The CMOR of specimen E1, for example, decreased from 19.73 MPa to 12.29 MPa, but for specimen EA0.5, from 19.43 MPa to 13.92 MPa. Namely, the residual strength ratio of CMOR of specimen was increased from 62.3 % to 71.7 % as 0.5 wt% ACG was introduced in Al_2O_3-C refractories. It is suggested that the alumina coating prevented the structural alteration of the expanded graphite. Much more residual graphite produced higher residual flexural strength and residual strength ratio.

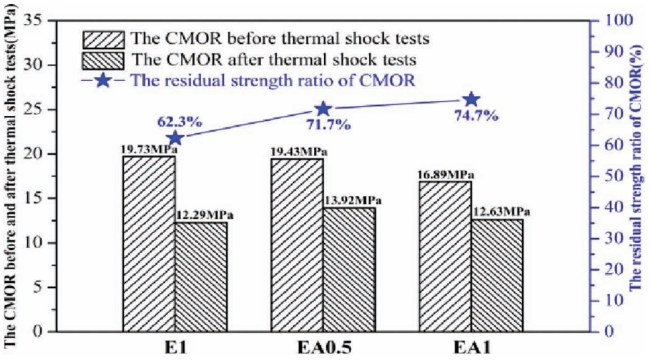

Fig. 9: Residual CMOR and their residual strength ratio of the specimens coked at 1200 °C after five thermal shock cycles.

IV. Conclusions

(1) Alumina-coated graphite (ACG) was successfully prepared in a process of soaking, filtering, drying and coking. The alumina coating on the surface of graphite delayed the oxidation behavior of the expanded graphite.

(2) ACG possessed a relatively integral structure of graphite as it was incorporated into Al_2O_3-C refractories after coking at high temperature. As a result, it could improve the thermal shock resistance of Al_2O_3-C refractories.

Acknowledgments

The authors are grateful for the financial support from the National "973" Project of China (2014CB660802), the Natural Science Foundation of China (51372176, 51574186).

References

1 Takanaga, S., Ochiai, T., Tamura, S., *et al.*: The application of the nano structural matrix to MgO-C bricks (Nano-tech. refractories-2) in: Proceedings of UNITECR'03 Congress, Osaka, Japan, (2011).

2 Yu, M.F., Lourie, O., Dyer, M.J, *et al.*: Strength and breaking mechanism of multiwalled carbon nanotubes under tensile load, *Science*, **287**, 637 – 640, (2000).

3 Luo, M., Li. Y.W., Jin, S.L., *et al.*: Microstructures and mechanical properties of Al_2O_3-C refractories with addition of multi-walled carbon nanotubes, *Mat. Sci. Eng. A*, **548**, 134 – 141, (2012).

4 Zhu, T.B., Li, Y.W., Sang, S.B., *et al.*: Effect of nanocarbon sources on microstructure and mechanical properties of MgO-C refractories. *Ceram. Int.*, **40**, 4333 – 4340, (2014).

5 Mahato, S., Pratihar, S.K. *et al.*: Fabrication and properties of MgO-C refractories improved with expanded graphite, *Ceram. Int.*, **40**, [10], 16535 – 16542, (2014).

6 Wang, Q.H., Li, Y.W., Sang, S.B., *et al.*: Effect of the reactivity and porous structure of expanded graphite (EG) on microstructure and properties of Al_2O_3-C refractories, *J. Alloy. Compd.*, **645**, 388 – 397, (2015).

7 Zhu, T.B, Li, Y.W., Jin, S.L. *et al.*: Microstructure and mechanical properties of MgO-C refractories containing expanded graphite. *Ceram. Int.*, **39**, 4529 – 4537, (2013).

8 Xu, X.F., Li, Y.W., Wang, Q.H. *et al.*: Effect of silicon-modified expanded graphite on microstructure and mechanical properties of Al_2O_3-C refractories, *Journal of Synthetic Crystals*, **45**, [9], 2257 – 2264, (2016).

9 Cheng, M., Yang, R., Zhang, L., *et al.*: Restoration of graphene from graphene oxide by defect repair, *Carbon*, **50**, [7], 2581 – 2587, (2012).

10 Shirasaki, T., Derré, A., Ménétrier, M., *et al.*: Synthesis and characterization of boron-substituted carbons, *Carbon*, **38**, [10], 1461 – 1467, (2000).

11 Sheng, Z.H., Shao, L., Chen, J.J., *et al.*: Catalyst-free synthesis of nitrogen-doped graphene via thermal annealing graphite oxide with melamine and its excellent electrocatalysis, *ACS Nano*, **5**, [6], 4350, (2011).

12 Wu, G.S., Ma, L.C., Liu, L., *et al.*: Preparation of SiO_2-GO hybrid nanoparticles and the thermal properties of methylphenylsilicone resins/SiO_2-GO nanocomposites, *Thermochim. Acta*, **613**, 77 – 86, (2015).

13 Kim, K.T., Dao, T.D., Han, M.J., *et al.*: Graphene coated with alumina and its utilization as a thermal conductivity enhancer for alumina sphere/thermoplastic polyurethane composite, *Mater. Chem. Phys.*, **153**, 291 – 300, (2015).

14 Wang, Q.H. Composition, microstructure and mechanical properties of Al_2O_3-C refractories containing expanded graphite: [D]. Wuhan: Wuhan University of Science and Technology, 2015.

15 Sumita, R., Mukesh, K., Sumit, S., *et al.*: Role of graphene in structural transformation of zirconium oxide. *J. Sol-Gel Sci. Techn.*, **71**, [3], 470 – 476, (2014).

16 Sitko, R., Turek, E., Zawisza, B., Adsorption of divalent metal ions from aqueous solutions using graphene oxide, *Dalton T.*, **42**, [16], 5682. (2013).

17 Park, S., An, J., Piner, R.D., Jung, I., *et al.*: Aqueous suspension and characterization of chemically modified graphene sheets, *Chem. Mater.*, **20**, [21], 6592, (2008).

18 Chen, W., Yan, L., Bangal, P.R.: Preparation of graphene by the rapid and mild thermal reduction of graphene oxide induced by microwaves, *Carbon*, **48**, [4], 1146 – 1152, (2010).

19 Ning, X.A., Li, K., Li, R.S., *et al.*: FTIR analysis of polyaluminium chloride, *Environ. Chem.*, **27**, [2], 263 – 26, (2008).

20 Li, X.J., Jiang, W.H., Wei, H.Y., *et al.*: FTIR analysis of metal chlorinated alcohol salt, *Guangzhou Chemistry*, **33**, [4], 42 – 47, (2008).

21 Shek, C.H., Lai, J.K.L., Gu, T.S.: Transformation evolution and infrared absorption spectra of amorphous and crystalline nano-Al_2O_3 powders, *Nano Structured Materials*, **8**, 605, (1997).

22 Zhang, C.S., Zhao, F., Zhang, J.J., *et al.*: Infrared spectroscopy of nano-sized alumina, *ACTA Chim. Sinica*, **57**, [3], 275 – 280, (1999).

23 Li, D.Y., Yang, H., Xie, T.T., *et al.*: The heat treatment process of hydrous alumina and characteristics of nanometer Al_2O_3, *Chinese J. Inorg. Chem.*, **22**, [1], 96 – 100, (2006).

24 Wang, Q.H., Li, Y.W., Luo, M., *et al.*: Strengthening mechanism of graphene oxide nanosheets for Al_2O_3-C refractories, *Ceram. Int.*, **40**, [1], 163 – 172, (2014).

25 Wang, H., Li, Y.W., Zhu, T.B., *et al.*: Microstructures and mechanical properties of Al_2O_3-C refractories with addition of microcrystalline graphite, *Ceram. Int.*, **40**, [7], 11139 – 11148, (2014).

26 Luo, M., Li, Y.W., Jin, S.L., *et al.*: Microstructures and mechanical properties of Al_2O_3-C refractories with addition of multi-walled carbon nanotubes, *Mat. Sci. Eng. A*, **548**, [5], 134 – 141, (2012).

27 Han, J.H., Cho, K.W., Lee, K.H., *et al.*.: Porous graphite matrix for chemical heat pumps, *Carbon*, **36**, [12], 1801 – 1810, (1998).

28 Zhao, J.G., Shi, J.L., Guo, Q.G., *et al.*: Carbon nanotube growth in the pores of expanded graphite by chemical vapor deposition, *Carbon*, **47**, 1747 – 1751, (2009).

29 Li, Y. W., Wang, Q. H., Fan, H. B.: Synthesis of silicon carbide whiskers using reactive graphite as template, *Ceram. Int.*, **40**, 1481 – 1488, (2014).